Frequency curves of meteorites

by E. A. Kreiken

(Department of Astronomy, Ankara University)

Özet: Enstitüde, her gün küçük miktarda demir tozlarının arz üzerine düştüğü görülmüştür. Cali hazırda, bu demir tozla-ının menşei belli değildir. Atmosferdeki bu tozlar, rüzgârla kumların aşınmasından ileri gelmiş olup, tamamen atmosferik bir hadise olabilir. Veya bn tozlar arz dışı menşeli olup meteorlarla alâkalı olabilirler. Bunlardan hangisi olduğuna hüküm vermek için bir kriteryum, demir tozlarının günlük miktarının mevsimsel değişimlerinin meteorların mevsimsel değişmelerine tekabül edip edemodiğine bakmaktır.

Hem vizüel olarak rasad edilen hem de gündüz zamanı rasad edilen meteorların hesaba alınması lâzımdlr. Whipple tarafından yapılan fotografik araştırmalar ve Radio Astronomide elde edilen neticeler (Lovell, Clegg, Porter, Prentice a. o) meteorların güneş sisteminin daimî azaları olduğu ihtimalini gittikçe arttırmasına rağmen, meteorların menşeleri katiyetle bilinmemektedir. Bu makaledeki üç ayrı eğri serisi, şu kabuller esas alınarak hesaplanmıştır.

A. Meteorlar kozmik menşelidirler.

B. Mcteorlar gbneş sisteminin azalarıdırlar ve ekliptik düzleminin içinde veya yakınında yörüngeler çizerler.

C. Meteorlar güneş sisteminin daimî azalarıdır ve güneş ekvator düzleminid içinde veya civarında yörüngeler.

Hesaplanan eğrilerin bazı önemli karakterleri incelenmiştir.

Abstract

It was found at this Institute that daily small amounts of iron dust fall on the surface of the earth. At present the origin of this iron dust is still unknown. It may be a purely atmospheric phenomenon, the iron dust in the atmosphere being due to wind and sand erosion. It also may be that the iron dust is of extra-terrestial origin and is related to the meteors. One of the criteria on which the decision depends is whether or not the seasonal changes in the diurnal amount of iron dust correspond with those of the meteorites.

With the meteorites both the visually observed and the day time meteors must be taken into account. The origin of the meteors is not known with absolute certainty, though the fotographic researches by Whipple and the result obtained in radio astronomy (Lovell, Clegg, Porter, Prentice, a.o.) have made it increasingly probable that the meteors are permanent members of the solar system.

Still in this paper three different sets of curves are computed which are based on the assumptions:

A. The meteors are of cosmic origin;

B. The meteors are members of the solar system and describe orbits in or near the plane of the ecliptic;

C. The meteors are permanent members of the solar system which describe orbits in or near the plane of the solar equator.

Some significant characteristics of the computed curves are discussed.

§ 1. Introduction.

At the beginning of this year it was observed at this Institute, that daily small particles of iron are falling on the surface of the earth. In February 1954 A. Kızılırmak started a series of observations in order to determine the amount of iron dust which falls per unit square surface and to ascertain whether any seasonal changes can be observed. In due course he will report about his observations.

As yet the origin of these iron particles is unknown. The iron particles may be related to meteorites, but the possibility that their origin is terrestial cannot a priori be discarded, especially on the dry Anatolian plateau with its many rock formations with iron contents. The seasonal changes which seem to be present may give some information. If the seasonal trends in the appearance of the iron dust coincides with the trends in the occurrence of meteorites, this might suggest a cosmic origin. At present such a comparison of the two trends is still impossible.

When the observations, which are now being carried out at this Institute for the iron dust, will be completed, the curve for the seasonal change of the amount of iron dust will become known. It will be difficult to obtain a similar curve for meteorites.

For the visually observed meteorites such a curve has been given by Whipple [1] a. o. However, from the observations of Clegg and Lovell [2] it can not be doubted, that the visually observed meteorites form only a part of the total numbers. It may be that the majority of the meteorites falls during day time and the curve for the total numbers might deviate from that obtained from the night meteorites. Therefore in the present article an attempt is made theoretically to determine the curves valid for the meteorites. In this we are confronted by the difficulty that the origin of the meteorites is not known with absolute certainty. Therefore various possibilities are being considered and curves are computed corresponding to these various possibilities. The following cases are considered:

A. The meteorites are of cosmic origin. As a result of the velocity of the sun through space, successive layers of particles in the surrounding cosmic cloud are drawn into the solar sphere of attraction and forced to describe an orbit around the sun.

B. The meteorites are moving around the sun in closed orbits which are confined to or are near to the plane of the ecliptic.

C. The meteorites are moving around the sun in closed orbits which are confined to or are near to the plane of the solar equator.

§ 2. The orbits of meteorites from interstellar space. (figure 1).

We first consider the case A. Let the velocity of the sun, relative to the surrounding cosmic clouds, be $V_\odot$ and let relative to the sun the celestial coordinates of the Apex of this solar motion be λ'_0 and β'. For computing the orbits of the particles around the sun, the sun may be considered to be at rest at the origin, while the particles approach the sun with a velocity $V_\odot$ which at infinite distance is parallel to the direction from the Apex to the sun.

In the gravitational field of the sun the particles describe an orbit which is given by the usual relation:

$$r = \frac{h^2/\mu}{1 + e \cos(\theta - 180)} \tag{1.2}$$

while the velocity is found from

$$V = V_{\odot} + \frac{2\mu}{r} \qquad (2.2)$$

The particle passes through its perihelion at some point P on the extension of the line connecting the origin and the Apex.

At perihelion distance we have

$$V_P^2 = V_{\odot}^2 + \frac{2\mu}{R_P}; \quad h^2 = R_P^2 \cdot V_P^2 \text{ and } R_P = \frac{h^2/\mu}{1+e} \cdots (3.2)$$

where V_P is the velocity at perihelion and R_P the perihelion distance. So for a particle which passes through a given perihelion distance R_P in virtue of (1.2), (2.2) and (3.2) we have:

$$e = R_P \cdot \frac{V_{\odot}^2}{\mu} + 1$$

and

$$r = \frac{R_P \cdot \left(R_P \frac{V_{\odot}^2}{\mu} + 2 \right)}{1 + \left(R_P \cdot \frac{V_{\odot}^2}{\mu} + 1 \right) \cos(\theta - 180)} \qquad \cdots (4.2)$$

Through any point of the ecliptic there will pass two streams of particles, an incoming and an outgoing, of which the velocities are equal but in opposite direction. For the particles which pass twice through the plane of the ecliptic the distances from the two points of intersection to the sun are unequal.

With sufficient accuracy the orbit of the earth can be considered to be circular. Consequently through each point of the earth's orbit also two streams of particles will pass, an incoming and an outgoing one. (see fig. 1). For the particles passing though the earth's orbit at longitude λ' the orbit is found from

$$\cos \theta_{\lambda} = \cos \beta \cos (\lambda' - \lambda'_0) \qquad \cdots\cdots (5.2)$$

and so if the distance of 1 A. U is represented by A, it follows from (4.2) that the perihelion distance of a particle which passes through the earth's orbit at longitude λ' is equal to:

$$R_{P,\lambda'} = \frac{\mu}{2 V_{\odot}^2} \left[- \left\{ 2 + \frac{A \cdot V_{\odot}^2}{\mu} \cos \beta \cos (\lambda' - \lambda'_0) \right. \right.$$

$$\left. \left. + \sqrt{\left\{ 2 + \frac{A \cdot V_{\odot}^2}{\mu} \cos \beta \cos (\lambda' - \lambda'_0) \right\}^2 + 4A \left\{ 1 - \cos\beta \cos(\lambda' - \lambda^0_0) \right\}} \right] \qquad (6.2)$$

The relative density of the stream of particles passing through the point λ' and the value of the angle θ_a which the direction of the radiant includes with the direction of the Apex are found in the following way.

From (4.2) and (5.2) it is evident that r becomes infinite for

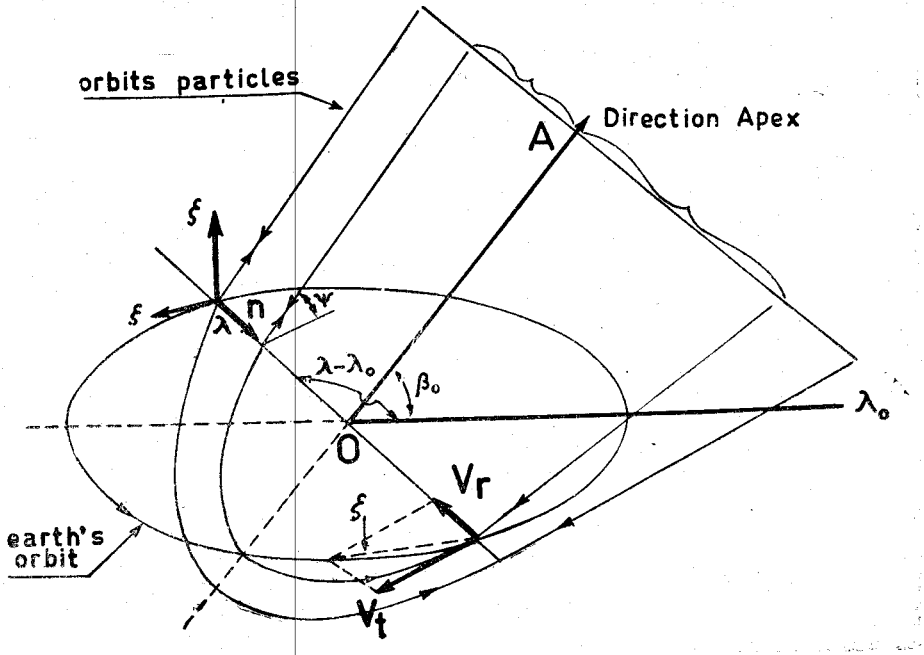

Fig. 1

$$\cos\theta_a = \frac{1}{R_{P,\lambda'}\frac{V_\odot^2}{\mu} + 1}$$

and therefore

$$\theta_a = \cos^{-1}\frac{1}{\left(1 + R_{P,\lambda'}\frac{V_\odot^2}{\mu}\right)} \qquad \cdots (7.2)$$

Now imagine a sphere of almost infinite radius, with the Apex as its pole. On the sphere we have a narrow circular band, defined by the angles θ_a and $\theta_a + d\theta_a$ The total number of particles passing through this belt is $C_1\, d \sin\theta_a/d\theta_a$ while C_1 and C_2 are constants.

Consequently the relative density of the stream of particles passing through λ' is

$$\rho = C \operatorname{cotg} \theta_a \qquad \cdots (8.2)$$

For the particles passing through λ' the radial and tangential velocities in the point λ' are:

$$V_R = \frac{\mu}{h} e \sin(\theta_\lambda - 180) = \mu \cdot \frac{\left(R_{P,\lambda} \cdot \frac{V_\odot^2}{\mu} + 1\right)}{R_{P,\lambda}\sqrt{\left(V_\odot^2 + \frac{2\mu}{R_{P,\lambda}}\right)}} \cdots (9.2)$$

$$V_t = \mu_h [1 + e \cos(\theta_\lambda - 180)] = \mu \frac{\left[1 + \left(R_{P,\lambda}\frac{V_\odot^2}{\mu} + 1\right) \cos\theta_\lambda\right]}{R_{P,\lambda}\sqrt{\left(V_\odot^2 + \frac{2\mu}{R_{P,\lambda}}\right)}} \quad (10.2)$$

Obviously the radiant of the particles passing through the point λ' does not coincide with the Apex. At any point λ' the angle between the direction of the velocity and the direction of the Apex is $\theta_\lambda \pm 90°$. Consequently the angle ξ included between the direction of the radiant and that of the Apex is equal to:

$$\zeta = \theta_\lambda \pm 90 + \tan^{-1}\frac{V_R}{V_t} \qquad \cdots (11.2)$$

In any point λ' the tangential velocity is perpendicular to $\overline{\lambda' O}$ and in the plane through λ' and the axis OA. The components of V_t in the plane of the ecliptic and perpendicular to this plane are $V_t \cos \Psi$ and $V_t \sin \Psi$ where the angle Ψ is easily found from spherical trigonometry. Therefore we can now find the three components of the total velocity $V\xi'$, $V\eta'$ and $V\zeta'$ relatively to a system of coordinates which is fixed ad λ'.

As for the earth a circular orbit has been assumed, the velocity of the earth in its orbit will be

$$V_E = \sqrt{\frac{\mu}{A}}$$

So the components of the velocities of the particles relatively to the earth will be:

$$V\xi = V\xi' - \sqrt{\frac{\mu}{A}}; \; V_r = V_r' \text{ and } V\zeta = V\zeta' \cdots (12.2)$$

The celestial longitude and latitude of the apparent radiants now will be:

$$\lambda_R' = \lambda + 90 + \mathrm{tg}^{-1}\frac{V_n}{V_\xi} \qquad \cdots\cdot (13.2)$$

and

$$\beta_R' = \cos^{-1}\sqrt{\frac{V_\xi^2 + V_\eta^2}{V_\xi^2 + V_\eta^2 + V_\zeta^2}} \qquad \cdot\cdot (14.2)$$

Passing from heliocentric coordinates λ' and β' to the geocentric coordinates λ and β by the usual relations

$\sin\delta = \sin\beta\cos\varepsilon + \cos\beta\cos\varepsilon\sin\lambda$ and $\cos\delta\cos\alpha = \cos\beta\cos\lambda$ (ε = obliquity of the ecliptic) the R. A and declination of the apparent radiants are found.

§ 3. Some numerical results.

The relations discussed in section 2 can only be applied if the velocity of the interstellar cloud relatively to the sun is given. For the present it is assumed that the velocity of the cloud is zero with respect to the local system of rest.

It should be realised that it is quite possible that the cosmic cloud surrounding the sun has a peculiar velocity. As a matter of fact Hoffmeister [3] thinks that there are some indications that such a peculiar velocity exists. However, as long as no more definite data are known, the best thing to do is to assume that the velocity of the cloud merely is the reflected solar velocity.

Consequently for $V_\odot$ the value $V_\odot = 20$ Km/sec. was adopted and for the coordinates of the Apex the values $\alpha = 270^\circ$ and $\delta = +34^\circ$. Then $\lambda_0 = 270^\circ$ and $\beta_0 = 57^\circ$ (fig. 1)

First from the relation (6.2) we compute the perihelion distance $R_{P,\lambda}$ for the particles passing through the earth's orbit at a point of longitude λ'. Next $\cos\theta_\alpha$ is computed from (7.2), while the relative stream density ρ is obtained from (8.2) where c is taken equal to 1. The phase angle θ_λ is found from (5.2). The results appear in table 1.

By inserting the values given in table 1 in the equations (9.2) and (10.2) we next find the values of the radial and the tangential velocities as given in table 2. The value of ζ as com-

Table 1.

Column 1 value of $\lambda' - \lambda_0'$
Column 2 celestial longitude λ' (heliocentric)
Column 3 celestial longitude λ (geocentric)
Column 4 Perihelion distance $R_{p\lambda}$ for particles passing throuh λ (form 6.2)
Column 5 Asymptote $\cos\theta_a$ for particles passing through λ (form 7.2)
Column 6 Stream densities ρ of particles passing through λ (form 5.2)
Column 7 Value of $\theta\lambda$ for different values of λ (form 5.2)

$\lambda' - \lambda_0'$	λ'	λ	$R_{p,\lambda}$	$\cos\theta_a$	ρ	$\theta\lambda$
0°	270°	90°	0.24	0.92	2.36	57°
30	300	120	0.27	0.92	2.36	62
60	330	150	0.36	0.89	1.96	74
90	0	180	0.48	0.80	1.33	90
120	30	210	0.62	0.72	1.04	106
150	60	240	0.72	0.67	0.90	118
180	90	270	0.75	0.65	0.85	123
210	120	300	0.72	0.67	0.90	118
240	150	330	0 62	0.72	1.04	106
270	180	0	0.48	0.80	1.33	90
300	210	30	0.36	0 89	1.96	74
330	240	60	0.27	0.92	2.36	62

Table 2.

Radial velocity V_R fordifferent values of $\lambda' - \lambda_0'$ (form. 9.2) Tangential velocity V_t for different values of $\lambda' - \lambda_0'$ (form. 10.2) Radiant of incoming stream ζ (form. 11.2) The angle ψ

$\lambda' - \lambda_0'$	V_R (Km/sec)	V_t (Km/sec)	ζ	ψ
0°	33.5	19.7	27°	90°
30	33.4	19.8	33	72
60	32.8	24.1	36	60
90	30 5	28.3	48	57
120	27.4	32.4	56	60
150	24.2	35.6	62	72
180	22.0	36.2	64	90
210	24,2	35.6	62	72
240	27.4	32.4	56	60
270	30.5	28.3	48	57
300	32.8	24.1	36	60
330	33.4	19.8	33	72

puted from (11.2) also appears in table 2, while the final column of this table gives the angle Ψ (fig. 1).

The next step is to compute the rectangular components $V\xi'$, V_r' and $V\zeta'$ of the two streams of particles and the components of the velocity $V\xi$, V_r and $V\zeta$ relative to the earth (12.2). The total relative velocity relative to the earth is $V^2 = \sqrt{V\xi^2 + V_h^2 + V\zeta^2}$ The results appear in table 3.

Table 3.

The three components $V\xi'$, V_r and $V\zeta'$ of the stream velocities relative to a system of coordinates fixed at λ (fig. 1).
The three components $V\xi$, V_r and $V\zeta$ relative to the earth.
The total velocity V relative to the earth.

$\lambda'-\lambda_0'$	$V\xi'$	V_n'	$V\xi'$	incoming stream				outgoing stream			
				$V\xi$	V_n	$V\zeta$	V	$V\xi$	V_r	$V\zeta$	V
0	0.0	−33.5	−19.7	−29.8	−33.5	−19.7	48.5	−29.8	+33.5	+19.7	48.5
30	+ 6.1	−33.4	−18.8	−23.7	−33.4	−18.8	44 6	−35.9	+33.4	+18.8	52 0
60	+11.8	−32.8	−21 0	−18.0	−32.8	−21.0	42.6	−41.6	+32.8	+21.0	56.4
90	+15.3	−30.5	−23 8	−14.5	−30.5	−23.8	41.0	−45.1	+31.5	+23.8	58.8
120	+15.9	−27.4	−28.2	−13.9	−27.4	−28.2	41.4	−45.7	+27.4	+28.2	59.7
150	+11.0	−24.4	−33 8	−18.8	−24.4	−33.8	45.4	−40.8	+24.4	+33.8	57.7
180	0.0	−22.0	−36.2	−29.8	−22.0	−36.2	51.3	−29.8	+22.0	+36.2	51.3
210	−11.0	−24.4	−33.8	−40.8	−24.4	−33.8	57.7	−18.8	+24.4	+33.8	45.4
240	−15.9	−27.4	−28.2	−45.7	−27.4	−28.2	59.7	−13.9	+27.4	+28.2	41.4
270	−15.3	−30.5	−23.8	−45.1	−30.5	−23.8	58.8	−14.5	+30.5	+23.8	41.0
300	−11.8	−32.8	−21·0	−41.6	−32.8	−21 0	56.4	−18 0	+32.8	+21.0	42.6
330	− 6.1	−33.4	−18 8	−35.9	−33.5	−18.8	52.0	−23.7	+33.5	+18.0	44.6

The next point is to compute the angle Δ_i between the radiant of the incoming stream and the instantaneous vertex of the earth's motion. These values appear in table 4. For the outgoing stream of particles the corresponding value is given in the column Δ_0. The next two columns in this table contain the angular distance c_i and c_0 from the radiants of the incoming and outgoing stream to the Apex. Finally β_i; β_0; λ_i and λ_0 indicate the celestial (geocentric) longitudes and latitudes of the radiants.

These celestial coordinates are converted in right ascension and declination and appear in the tables 5 and 6. In these tables 5 and 6 all data concerning the incoming and outgoing

streams are collected. The values of the velocity V are taken from table 3. The number of particles which are swept up by the earth per unit of time is proportional to the product $\rho \cdot V$ These values $\rho \cdot V$ also appear in the tables.

For $\rho \cdot V$ the smallest numerical value is 40.9 and dividing all values $\rho \cdot V$ by 40.9 we find the relative activity of the radiants in different times of the year. From the right ascensions as given in column 3 it is not difficult to find at what time (universal time) the radiant passes through the observer's meridian. The numerical values of the U. T are given in the final column of the tables 5 and 6.

Table 4.

The angles Δ_i and Δ_0 are the angles between the apparent radiant and the instantaneous vertex of the earth's motion.

The celestial latitudes β_i and β_0 of the radiants

The celestial longitudes λ_i and λ_0 of the radiants

c_i and c_0 represent the angular distance from the radiants to the Apex

$\lambda'-\lambda_0'$	Δ_i	Δ_0	β_i	β_0	c_i	c_0	λ_i	λ_0
0°	52.4°	52.4°	+24.5°	−24.5°	40.5°	40.5°	310.5°	49.5°
30	58.0	46.5	+24.5	−21.5	34.9	46.4	334.9	73.7
60	65.2	42.3	+29.5	−21.5	27.1	50.9	357.1	99.1
90	69.5	39.6	+35.9	−23.1	24.5	55.3	24.5	127.7
120	70.1	40.5	+43.1	−28.3	25.8	58.7	55.8	151.3
150	65.8	44.8	+47.9	−35.9	36.8	58.7	96.8	181.3
180	54.5	54.5	+44.7	−44.8	53.1	53.1	143.1	216.9
210	44.8	65.8	+35.9	−47.9	58.7	36.8	178.7	263.2
240	40.5	70.1	+28.3	−43.1	58.7	25.8	208.7	304.2
270	39.6	69.5	+23.0	−34.9	55.3	24.5	235.3	335.5
300	42.3	65.2	+21.5	−29.5	50.9	27.1	260.9	2.9
330	46.5	58.0	+21.5	−24.5	46.4	34.9	286.4	25.2

§ 4 Discussion of the numerical results obtained in section 3.

From the tables 5 and 6 it appears that if supposition A is correct, there will be a seasonal variation of the relative abundancies of meteorites. This appears more clearly from figure 2, where the relative abundancies have been plotted against time. There is a flat maximum during the summer months and a mi-

Table 5.

Collected informations about the incoming stream (stream from North). Date, coordinates α and δ of the apparent radiant, the product ρV (section 5) the relative activity of the radiant and approximate Universal time of meridian passage of the radiant.

$\lambda' - \lambda_0'$	Appr. Date	α	δ	V (Km/sec)	ρV	A	u. T
0°	June 21	306°	+ 6°	48.5	114.5	2.8	$2^1/_2{}^h$
30	July 21	328	+13	44.6	105.3	2.6	2
60	Aug. 21	355	+26	42.6	83.5	2.0	$1^1/_2$
90	Sept. 21	0	+42	41.0	54.5	1.3	0
120	Oct. 21	39	+58	41.4	43.1	1.1	$^1/_2$
150	Nov 21	105	+70	45.4	40.9	1.0	3
180	Dec. 21	168	+54	51.3	43.6	1.1	5
210	Jan. 21	196	+33	57.7	51.9	1.2	5
240	Febr. 21	215	+19	59.7	62.1	1.5	$4^1/_2$
270	Mar. 21	230	+ 4	58.8	78.2	1.9	$3^1/_2$
300	Apr. 21	261	— 1.3	56.4	110.5	2.7	$3^1/_2$
330	May 21	285	— 0.6	52.0	122.7	3.0	3

Table 6.

Collected informations about the outgoing stream (stream from South Compare with table 5)

φ	Appr Date	α	δ	V Km/sec	ρV	A	u. T	$A_i + A_i$
0°	June 21	49°	— 6.0°	48.5	114.5	2.8	$9^1/_2{}^h$	5.6
30	July 21	75	+ 0.5	52.0	122.7	3.0	9	5.6
60	Aug 21	99	+ 1.1	56.4	110.5	2.7	$8^1/_2$	5.7
90	Sep. 21	124	— 4	58.8	78.2	1.9	$8^1/_2$	3.2
120	Oct. 21	145	—16	59.7	62.1	1.5	8	2.6
150	Nov. 21	164	—33	57.7	51.9	1.2	7	2.2
180	Dec. 21	194	—54	51.3	43.6	1.1	7	2.2
210	Jan. 21	259	—64	45.4	40.9	1.0	9	2.2
240	Feb. 21	305	—59	41.4	43.1	1.1	11	2.6
270	Mar. 21	354	—42	41.0	54.5	1.3	$11^1/_2$	3.2
300	Apr. 21	14	—26	42.6	83.5	2.0	11	5.7
330	May. 21	31	—13	44.0	105.3	2.6	10	5.6

nimum during the winter months. In figure 2 however the geographic latitude of the observer has not been taken into account.

A more complete survey of the results of the computations is given in figure 3.

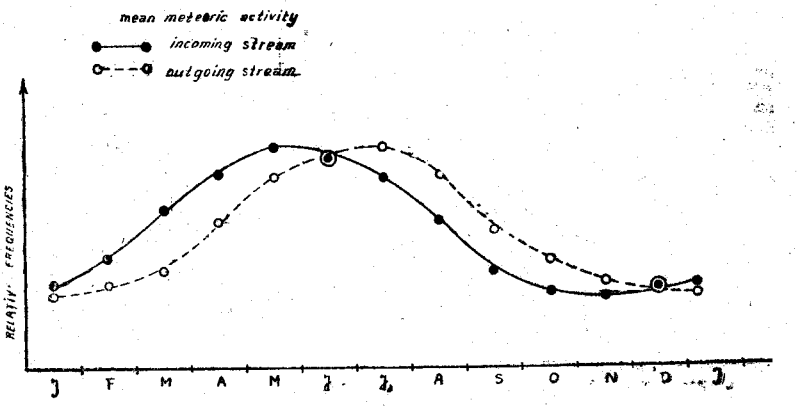

Fig. 2. Relative Frequency of meteorites in different months of the year for case A.e g. origin of meteorites is cosmic and cloud surrounding the sun has zero velocity with respect to the local rest system.

This figure gives the positions of the radiants in different parts of the year.

The surface of the open circles and dots is proportional to the relative abundancy of the radiants. The arrows indicate the velocity with which the meteorites approach the earth.

For meteorites of cosmic origin all orbits must be hyperbolic ones. In many cases however, the computed velocities relative to the earth are very near the escape velocity. If for the velocity of the sun a slightly different value is assumed, the computed relative velocities would be such as to suggest closed orbits rather than parabolic or hyperbolic ones.

In figure 3 the radiant of meteors, having a velocity which is nearly equal to the escape velocity, are indicated by open circles and as possible closed orbits.

Between June and December all meteorites from radiants North of the ecliptic would be difficult to distinguish from meteors describing closed orbits, but in the remaining months of the year the velocities of the meteorites would be such, that hyperbolic orbits would be obtained.

In a similar way the meteorites from Southern radiants be-

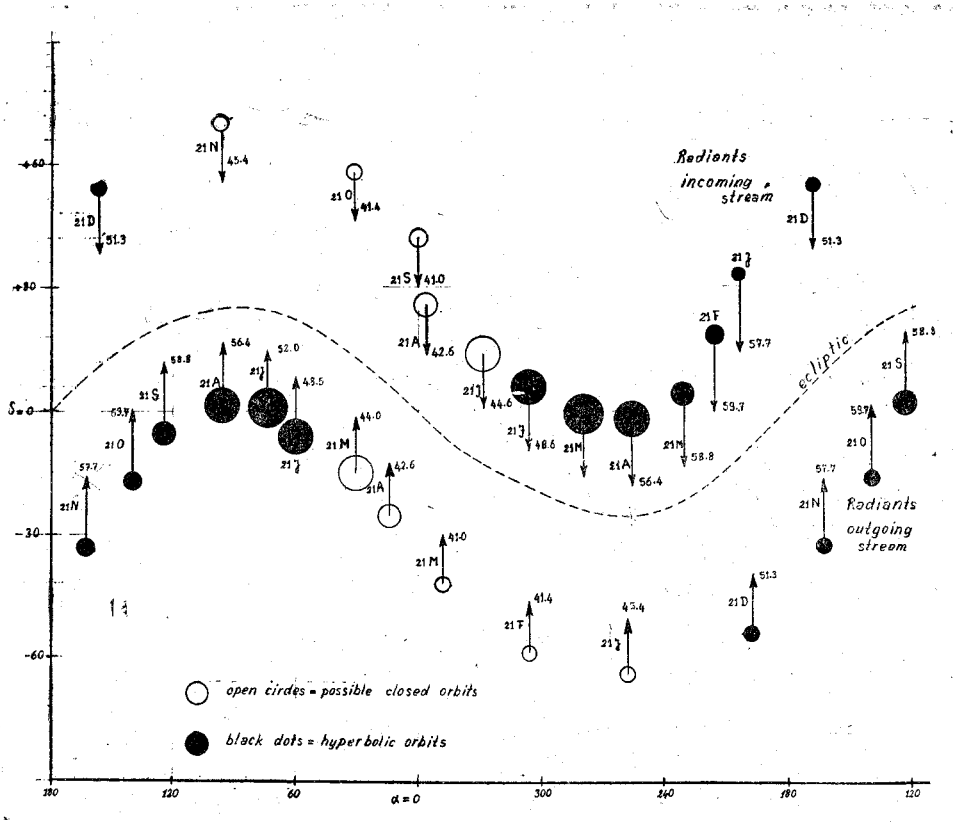

Fig. 3: Position of the Radiants in different parts the year. (Supposition A)

tween January and June would appear to move along closed orbits.

There seems to be a striking resemblance between our figure 3 and the one given by Lovell and Clegg in their book on Radio-Astronomy[4] for the radiants of the visually observed and the day time meteor showers. In both cases the radiants seem to be confined to rather narrow belts North and South of the ecliptic, while there is a continuous increase of the right ascension of the radiant throughout the course of the year.

In addition to this it appears from the tables 5 and 6 that radiants from cosmic origin as suggested by hypothesis A, will pass through the meridian either shortly after midnight or shortly before noon. But these are exactly the instants at which Lovell and Clegg find maxima of meteoric activity[5].

The likeness between the two figures is however rather superficial and on closer scrutiny it appears to be impossible to associate the radiants of tables 5 and 6 and figure 3 with the observed radiants. It is worth while to consider this question in some details.

§ 5. The radiants of the observed showers.

Table 7 gives the positions of the radiants of the meteor showers which have been observed up till now. The showers, numbered from 1 — 10, have been visually observed and are recurrent ones.

The radiants 11 - 20 correspond to the major daytime showers which have been detected by radar observations[6]. The numbers 11, 12 and 13 are recurrent ones. The others (14 - 20) have not appeared regularly and Lovell and Clegg[7] state that there is not yet sufficient information to assess whether they are periodic or isolated occurrences.

Table 7 has been arranged in the following way. The first column gives the rotating number of the radiant and the second the date of its appearence. The third column gives the heliocentric longitude of the earth at that date. The next four colums give the right ascension, declination, celestial longitude and latitude respectively of the radiant.

The heliocentric longitude of the instantaneous vertex of the motion of the earth is equal to the earth heliocentric longitude + 90°. The difference between this longitude and the longitude

TABLE 7

Major meteor showers. 1 — 10 visually observed showers
11 — 20 daytime showers

N	Date	λ_s	α	δ	λ	β	Δ
1	Jan. 3	102°	230°	+ 52°	180°	+ 67°	— 12°
2	Apr. 21	210	270	+ 33	270	+ 56	— 30
3	May 6	225	338	+ 3	336	+ 11	— 21
4	July 28	304	339	— 11	336	— 2	— 58
5	Aug. 12	319	47	+ 58	57	+ 51	— 8
6	Oct. 21	27	96	+ 15	96	— 7	— 21
7	Nov. 6	43	55	+ 15	57	— 4	— 76
8	Nov. 16	53	152	+ 22	125	— 10	— 18
9	Dec. 14	81	113	+ 32	110	+ 11	— 61
10	Dec. 22	90	207	+ 77	203	+ 68	+ 23
11	June 3	252	61	+ 24	64	+ 4	+ 82
12	June 8	257	44	+ 23	50	+ 6	+ 63
13	July 2	280	86	+ 19	86	— 4	+ 76
14	May 10	229	26	+ 25	32	+ 13	+ 73
15	May 21	240	30	— 3	26	— 14	+ 56
16	June 25	273	68	+ 33	71	+ 11	+ 68
17	July 12	289	87	+ 11	87	— 12	+ 68
18	July 12	289	98	+ 21	97	— 2	+ 78
19	July 12	289	111	+ 15	110	— 6	+ 91
20	July 25	302	87	+ 38	88	+ 15	+ 56

of the radiant is $\Delta = \lambda_s + 90 - \lambda_R$ and is given in the last column of the table. From this last column it appears that for all but one (No. 10) of the visually observed showers, the velocity of the meteors is such that they approach the sun. On the other hand, as already remarked by Lovell and Clegg, all daylight showers come from the direction of the sun. The values of table 7 have graphically been represented in figure 4, where the showers are represented by arrows parallel to the direction from the radiant.

In each instance the arrow points to the instantaneous position of the earth in its orbit. The arrows, indicating the showers observed visually, are black, the others indicate the daytime showers discovered from radar observations. All arrows have been made to originate from a black dot or an open circle. Black dots indicate that the latitude of the radiant is positive and that the showers approach the ecliptic from the North.

Conversely open circles indicate that the latitude of the radiant is negative and that the shower approaches the plane of the ecliptic from the South. The numbers written along the arrows refer to the rotating number of the shower in table 7.

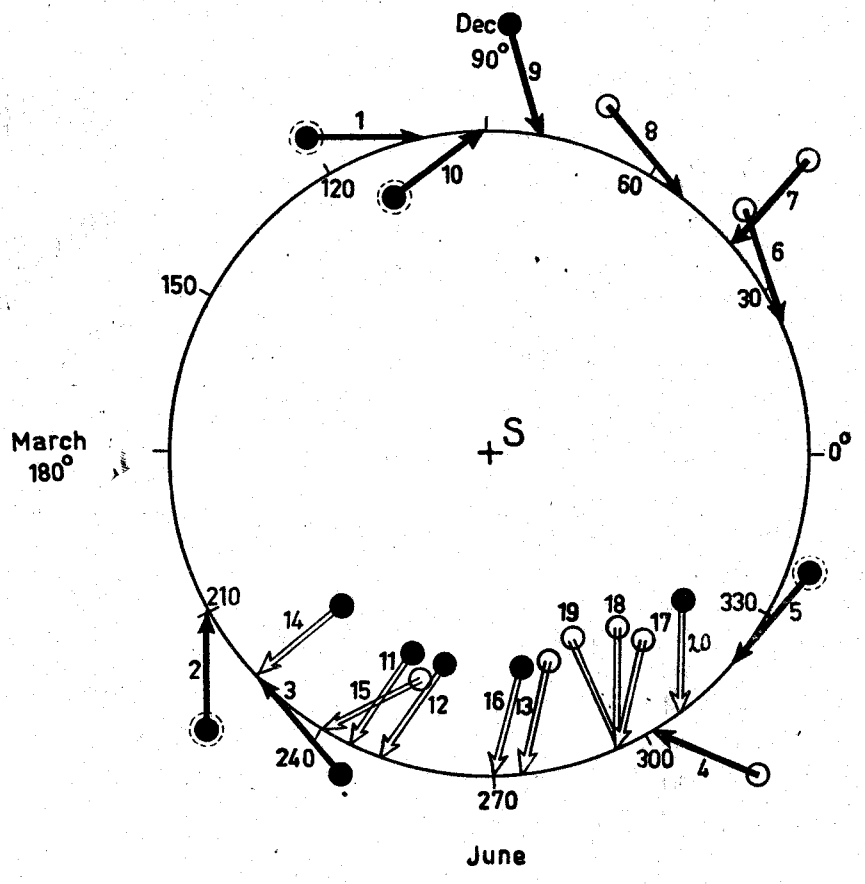

Fig. 4 The Observed Radiant of showers. Black arrows indicate showers which have visually been observed. White arrows indicate daytime showers. A black dot at the origin of the arrow indicates that the shower approaches the plane of the ecliptic from the north, open circles from the south. The numbers refer to table 7. The scale along the circle indicates the heliographic longitude of earth.

With hypothesis A all radiants of the incoming stream were North of the ecliptic, while shortly after midnight the radiant passed through the observer's meridian.

The radiants of the outgoing stream were South of the ecliptic, while the radiants passed through the meridian slightly before noon.

When we consider figure 4, it might appear at first sight that the distribution of the radiants of the major showers corresponds to the description given above and that therefore the occurrence of the major showers could be explained from the space motion of the sun. Both the incoming and the outgoing streams seem clearly to be indicated and there is a seasonal shift in the positions of the radiants while at the predicted times these radiants pass through the observer's meridian.

On closer scrutiny it becomes evident that there also are significant differences, which make it seem improbable that the major showers, either the recurrent or semirecurrent ones, are connected with streams from interstellar space.

First consider the latitudes of the radiants of the incoming showers. With streams from interstellar space all these latitudes would be positive. Of the observed incoming showers five have a positive and four a negative latitude.

With streams from interstellar space the radiant of the outgoing stream must have a negative latitude. Of the observed radiants of the outgoing streams, six have positive latitude, while the remaining have a negative latitude.

With the exception of the showers 1, 2, 5 and 10 all radiants are near the plane of the ecliptic and their distribution around this plane seems to be a haphazard one with a small standard deviation. This is even more apparent from fig. 5 in which the longitudes of the radiants have been plotted against their latitudes.

The full drawn curve indicates the relation between longitude and latitude for the incoming stream as computed in table 5, while the broken line gives this same relation for the outgoing stream (table 6). The observed radiants have been indicated by black dots (visually observed showers) and open circles (daylight showers). It is evident that neither set of radiants can be correlated to streams from interstellar space. For the majority of the showers the latitude is much smaller than the computed one. For the four showers 1, 2, 5 and 10 the observed latitude is considerably larger.

From figure 5 a peculiar feature in the distribution of the showers is evident, which is important for our considerations.

Obviously showers are observed only when the earth is between the heliocentric longitudes 210°-336° and 260-125°. In the intermediate intervals showers are markedly absent. It may be significant that the four peculiar showers 1, 2, 5 and 10 are exactly at the edges of the ranges where showers occur.

It seems hardly possible to ascribe this curious distribution to the influence of selection. The visual showers appear to be most frequent around November. Although a few appear shortly

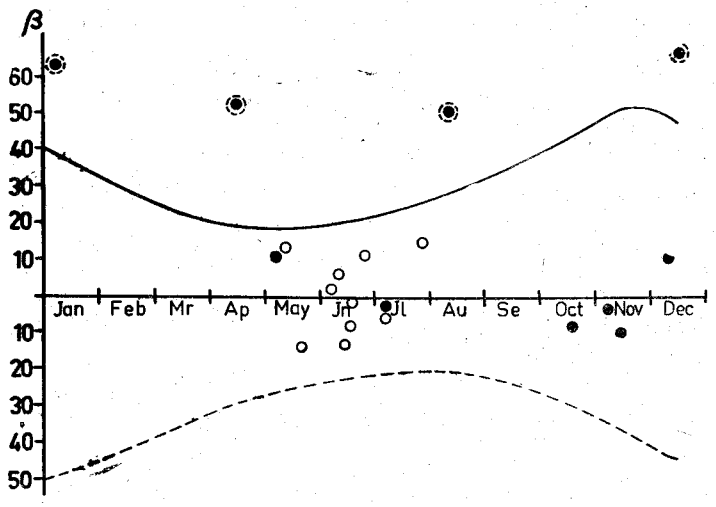

Fig. 5. Comparison of the observed and theoretical distribution of radiants.

before and after June, none are observed around February and September. Daylight showers seem to be limited to a short range of time before and after June. Lovell and Clegg[8] state (1. c. page 97) that a continuous and systematic survey was carried out without intermission throughout the year. No other outstanding showers have been found.

Therefore both the latitude distribution of the radiants and their distribution throughout the course of a year point to a non interstellar origin of the major showers. It is to be remarked that the earth intersects the plane of the solar equator when its heliocentric longitude is 75° and 255°.

The majority of the showers therefore seem to occur when

the earth is in or near the solar equatorial plane. They therefore may be connected with the streams of particles which revolve around the sun in its equatorial plane

§. 6 Frequency of meteors in different parts of the year and for different geographic latitudes for case A.

From section 5 it appears that it is not possible directly to connect the observed meteor showers with streams of particles from interstellar space which originate as stated in the supposition A.

Although no definite analysis has been made by the author, it does not seem that this conclusion can be invalidated by accepting other values for the velocity $V_{\odot}$ and for the coordinates of the Apex. This agrees with the conclusion which Lovell and Clegg[9] draw from the observed values of the velocities and which was also reached by Prentice[10] and Mc Kinley[11].

Still, when trying to decide whether the amount of iron which at this institute is observed daily to fall is either from terrestial or non-terrestial origin, the possibility that this iron dust, partly at least, is of cosmic origin should not be entirely discarded. From the computations it appeared that in many cases the velocities of such meteors were very near the limit of the escape velocity. As observed from the earth, they might appear to move in closed orbits.

In this improbable case the seasonal changes in the amount of iron dust, should correspond to the seasonal changes in the observable numbers of meteors.

For a comparison the curves in fig. 2 cannot be used. They indicate the relative abundancy of the two streams which approach the earth in the different months of the year, but not the relative frequencies of the meteors which will be observed. For this the reason is that the meteor frequency not only depends on the abundancy but also on the geographic latitude of the observer, that is on the zenith distance of the radiant.

For both the incoming and the outgoing stream the peak of meteoric activity occurs when the radiant passes through the observer's meridian, but also before and after this time some activity will occur. To find the general relation between the relative activity and the zenith distance we proceed in the same way as in section 2.

When proceeding in its orbit around the earth, a particle will pass through its perihelion at a point on the extension of the line connecting the true radiant and the center of the earth. This perihelion distance is found from (6. 2) by replacing $\mu = G M_{\odot}$ by $\mu' = G M_{earth}$ and $V_{\odot}$ by the stream velocity of the particles. For this a mean value $V = 50$ Km/sec. is adopted. Next the values θ_a and arg θ_a are found from (7.2) and (8. 2) in which also $V_{\odot}$ is replaced by $V = 50$ Km/sec.

When the particles collide with the atmosphere of the earth, their distance r from the center of the earth is $r = 1$.

Therefore the phase angle θ is found from (1, 2). Only such particles will collide with the earth's atmosphere for which the perihelion distance $r_P <$ radius earth. The relative frequency of the particles which, when penetrating into the atmosphere of the earth, have a phase angle θ, at the same time gives us the relative frequencies cotg θ_a (see 8. 2) of a radiant for which the zenith distance is θ.

The result of these calculations appear in table 8. The values cotg θ_a, as given in table 2, were plotted against the corresponding values θ and through the points obtained in this way a smooth curve was drawn. This curve is well determined up to the point $\theta = 16°$. Beyond this point its course is uncertain. It was supposed to intersect the axis cotg θ_a at the point cotg $\theta_a = 5.35$. This value cotg θ_a must be *considered as a mere guess*. It can only be accepted for the present because it does not have a large influence on the further results.

If, however, the radiant were a point source for $\theta = 0$, the value of cotg θ_a would tend to become infinite. The radiant will be a point source only when the particles have no peculiar velocities whatever. We have no information as to the distribution of these indivicual velocities and therefore as provisional value of cotg θ_a for $\theta = 0$ the value was adopted which from the shape of the curve seems to be the most probable one. Therefore the smoothed values of the relative frequencies F as given in table 9 must also be considered as provisional ones. If from further observations there will appear to exist a relation between the amount of iron dust and the hypothetical cosmic meteors, the values in table 9 will have to be more carefully calculated.

The amount of cosmic dust which from a radiant penetrates

TABLE 8

The values θ_a, cotg θ_a, cos θ and θ for particles striking the atmosphere of the earth and which would have a perihelion distance $r_p <$ radius earth.

r_p	θ_a	cotg θ_a	cos θ	θ
1.00	88°.6	0.024	−1.00	180°
0.80	88.3	.030	− .79	142
0.60	87.7	.040	− .58	126
0.40	86.6	.059	− .36	111
0.20	83.7	.110	− .06	94
0.15	82.0	.140	− .03	92
0.10	78.5	.204	+ .08	85
0.08	76.1	.248	+ .14	82
0.06	73.1	.30	+ .22	77
0.04	67.7	.41	+ .33	71
0.02	55.9	.68	+ .52	59
0.015	51.7	0.79	+ .60	53
0.010	44.8	1.01	+ .70	46
0.008	40.5	1.17	+ .74	42
0.006	35.9	1.38	+ .80	37
0.004	29.5	1.77	+ .85	32
0.002	21.6	2.53	+ .92	23
0.001	16.3	3.42	+ .96	16

TABLE 9

Smoothed values of the relative frequencies F.

θ	Rel. F.	θ	Rel. F.
0°	1.00	80°	0.05
5	0.97	85	04
10	.90	90	.03
15	.69	95	.02
20	.50	100	.02
25	.39	105	.02
30	.32	110	.01
35	.26	115	.01
40	.22	120	.01
45	.18	125	.01
50	.15	130	.01
55	.13	135	.00
60	.11	140	.00
65	.10	145	.00
70	.08	150	.00
75	.06	155	.00

into the atmosphere, depends on the abundancy A (tables 5 and 6) of the radiant and on the angular distance from the radiant to the zenith at this point. The coordinates α and δ of the apparent radiant vary systematically throughout the course of the year, thus causing a change of the zenith distance. Moreover, due to the diurnal rotation relatively to a fixed point on the earth, the position of the radiant varies constantly. If φ is the geographic latitude of this point and h the spherical angle between the meridian through this point and the meridian through the radiant, the instantaneous value of the zenith distance z is

$$\cos z = \sin \varphi \sin \delta + \cos \varphi \cos \delta \cos h \qquad (1.\ 4)$$

This instantaneous value of z is equal to the value of θ in table 9.

To find the total daily contribution of the radiants for a point at latitude φ, the values of z corresponding to different values of h are computed. For $\varphi = +60°$ an example is given in table 10. The first column in this table gives the declinations of the radiants, while the next two columns contain the corresponding values $\cos \varphi \sin \delta$ and $\cos \varphi \cos \delta$. For h the values 15°, 45°, 70°, 105°, 135° and 165° are adopted. For reasons of symmetry it is not necessary to consider the values of h between 180° and 360°. The values in table 10 are multiplied by cos 15, cos 45 etc. and so we obtain the values $\cos z$ as given in the next colums of the table. 10. From these values $\cos z$ we immediately find the corresponding values z as are entered in the final columns of table 10.

Consequently, using these values z from the curve given in table 9, we read the relative amount of cosmic dust falling at latitude φ when the declination of the radiant is δ and when $h = 15°, 45° \ldots$ and 135° respectively. These partial contributions ΔF appear in table 5. The total daily amount of cosmic dust contributed by a radiant at δ is proportional to $\Sigma \Delta F$ and is given in the final column of table 11.

Actually of course a continuous instead of discontinuous variation of the activity of a radiant will occur, but numerically the difference will be small. For the present at least it is sufficient only to consider discontinuous variations.

As the next step for different times of the year we tabulate the values of the incoming and outgoing radiants. These values

TABLE 10

Values of cos z and of z for different values of h. ($\varphi = +60°$)

δ	sin φ × sin δ	cos φ × cos δ	values of cos z for $h =$ 150°	$h =$ 45°	$h =$ 75°	$h =$ 105°	$h =$ 135°	$h =$ 160°	values of z for $h =$ 15°	$h =$ 450°	$h =$ 75°	$h =$ 105°	$h =$ 135°	$h =$ 165°
+70°	+.82	+.17	+.99	+.94	+.86	+.78	+.70	+.65	8	20	31	39	44	50
+60	+.76	+.25	+1.00	+.94	+.88	+.69	+.58	+.51	0	20	34	46	55	59
+50	+.67	+.32	+.98	+.89	+.75	+.59	+.45	+.36	11	27	41	54	63	69
+40	+.56	+.38	+.93	+.83	+.66	+.46	+.29	+.19	22	34	49	63	73	79
+30	+.44	+.43	+.85	+.75	+.55	+.33	+.13	+.02	31	41	57	71	83	89
+20	+.30	+.47	+.76	+.63	+.42	+.18	−.03	−.16	40	51	65	80	92	99
+10	+.15	+.49	+.63	+.50	+.28	+.02	−.20	−.33	51	60	74	89	102	109
0	.00	+.50	+.49	+.36	+.13	−.13	−.36	−.49	61	69	82	97	111	119
−10	−.15	+.49	+.33	+.20	−.02	−.28	−.50	−.63	71	79	91	106	120	129
−20	−.30	+.47	+.16	+.03	−.18	−.42	−.63	−.76	81	88	100	115	129	140
−30	−.44	+.43	−.02	−.13	−.33	−.55	−.75	−.86	91	97	109	123	139	149
−40	−.56	+.38	−.19	−.29	−.46	−.66	−.83	−.93	101	107	117	131	146	158
−50	−.67	+.32	−.36	−.45	−.59	−.75	−.89	−.98	111	117	126	139	153	169
−60	−.76	+.25	−.51	−.58	−.69	−.83	−.94	−1.00	121	126	134	146	160	180
−70	−.82	+.17	−.65	−.70	−.78	−.86	−.94	−.99	130	134	141	149	160	172

TABLE 11

Values of ΣF and $\Sigma \Delta F$ for different values of h ad δ ($\varphi = +60°$)

δ	ΔF						$\Sigma \Delta F$
	$h =$ 15°	$h =$ 45°	$h =$ 75°	$h =$ 105°	$h =$ 135°	$h =$ 165°	
+ 70	.90	.50	.32	.22	.18	.15	2.27
+ 60	1.00	.50	.26	.18	.13	.11	2.18
+ 50	.90	.39	.22	.13	.10	.08	1.82
+ 40	.50	.26	.15	.10	.06	.05	1.12
+ 30	.32	.22	.13	.08	.04	.03	0.82
+ 20	.22	.15	.10	.05	.03	.02	0.57
+ 10	.15	.11	.06	.03	.02	.01	0.38
0	.11	.08	.05	.02	.01	.01	0.28
— 10	.08	.05	.03	.02	.01	.01	0.20
— 20	.05	.03	.02	.01	.01	.00	0.12
— 30	.03	.02	.01	.01	.00	.00	0.07
— 40	.02	.02	.01	.01	.00	.00	0.06
— 50	.01	.01	.01	.00	.00	.00	0.03
— 60	.01	.01	.00	.00	.00	.00	0.02
— 70	.01	.00	.00	.00	.00	.00	0.01

are enumerated in tables 5 and 6. The values in table 12 are borrowed from this table and have been appoximated by the nearest multiple of 10.

On January 21st the approximate declination of the radiant of the incoming stream is $\delta_N = +10°$ while that of the outgoing is $-60°$. From table 11 we find that at latitude $= +60°$ the total daily contributions of the two radiants are proportional to $\Sigma \Delta F_N = 0.82$ and $\Sigma \Delta F_S = 0.02$ respectively.

From tables 5 and 6 we see that the relative activities of the radiants at this date are $A_N = 1{\cdot}2$ and $A_S = 1.0$ respectively. The total daily amounts of cosmic dust, contributed by the two radiants, therefore are proportional to $D_N = 0.82 \times 1.2$ and $D_S = 0.02 \times 1.0$ or $D = D_N + D_S = 0.98 + 0.02 = 1.00$.

For the other months we proceed in a similar way. The resulting curve appears in the last column of table 12. This curve therefore represents the relative amount of cosmic dust which at different times of the year penetrates into our atmosphere at a point at geographic latitude $+60°$. Our numbers are proportional to the total numbers of meteorites which penetrate into the atmosphere of the earth during a period of 24 hours. Of

TABLE 12

($\varphi = +60°$)

Date	δ_N	δ_S	$\Sigma\Delta F_N$	A_N	D_N	$\Sigma\Delta F_S$	A_S	D_S	$D = D_N + D_S$
Jan. 21	+30	−60	+ .82	1.2	.98	.02	1.0	.02	1.00
Febr. 21	+20	−60	+ .57	1.5	.86	.02	1.1	.02	.88
March 21	0	−40	+ .28	1.9	.53	.06	1.3	.08	.61
Apr. 21	0	−30	+ .28	2.7	.76	.07	2.0	.14	.90
May 21	0	−10	+ .28	3.0	.84	.20	2.6	.52	1.36
June 21	+10	−10	+ .38	2.8	1.06	.20	2.8	.58	1.64
July 21	+10	0	+ .38	2.6	.99	.28	3.0	.84	1.83
Aug. 21	+30	0	+ .82	2.0	1.64	.28	2.7	.76	2.40
Sept. 21	+40	0	+ 1.12	1.3	1.46	.28	1.9	.53	1.99
Oct. 21	+60	−20	+ 2.18	1.1	2.40	.12	1.5	.18	2.58
Nov. 21	+70	−30	+ 2.27	1.0	2.27	.07	1.2	.08	2.35
Dec. 21	+50	−50	+ 1.82	1.1	2.00	.03	1.1	.03	2.03

TABLE 13

Relative daily amount of cosmic dust in different latitudes φ and in different times of the year. (case A)

Date \ φ	+90°	+60°	+40°	+20°	0°	−20°	−40°	−60°	−90°
Jan. 21	0.78	1.00	1.68	1.14	.95	.83	1.31	2.18	1.98
Fabr. 21	.72	.88	1.38	1.37	1.26	1.14	1 55	2.40	2.22
March 21	.42	.61	.96	1.33	2.73	2.01	2.64	1.48	1.74
April 21	.60	.90	1.48	2.00	4.25	3.23	3.88	1.64	1 80
May 21	.84	1.36	2.10	2.85	5.95	3.42	2.85	.99	1.52
June 21	1.20	1.64	2.55	3.14	5.32	3 14	2.53	1.06	1.20
July 21	1.32	1.83	2.85	3.42	5.95	2.85	2.10	.84	.84
Aug. 21	1.80	2.40	3.88	3.23	4.25	2.00	1.48	.76	.60
Sept. 21	1.50	1.99	2.64	2.01	2.73	1.33	0.96	.53	.42
Oct. 21	2.22	2.58	1.55	1.14	1.26	1.37	1.38	.86	.72
Nov. 21	3.06	2.35	1.17	.83	0 90	1.14	1.68	.98	.78
Dec. 21	1.44	2.03	1.47	.90	0.74	.90	1.47	2.00	1.44
Σ	15.90	19.57	24.51	23.36	36.29	23.36	23.83	19.47	15.06

these meteors, however, the majority falls during daytime and can not visually be observed. Moreover, the fractions which are contributed by the two radiants to the daytime (sporadic) meteors are different from the fractions contributed to the (sporadic) meteors which appear during the night.

The numbers in table 12 are valid for the geographic latitude $\varphi = + 60°$ only.

The curves valid in the other latitudes are obtained in exactly the same way. They are given in table 13, which therefore needs no further explanation.

The numbers in the table are the numerical values of $D = D_N + D_S = A_N \Sigma \Delta F_N + A_S \Sigma \Delta F_S$ in the different latitudes φ.

For obtaining the true amounts of cosmic dust the values D must be multiplied with a certain constant. As the numerical value of this constant is unknown, at present only the relative values can be considered.

When deriving the coordinates α and δ of the radiants, it has been assumed that the cloud of particles surrounding the sun has no peculiar motion. Also the particles in the cloud were supposed to have no individual velocities. Therefore all numerical values given in table 13 are based on these same assumptions.

§ 7. Case B.

It is next assumed that all meteors move in closed orbits around the sun, while the plane of this orbit is in or near the plane of the ecliptic. If the distribution of the particles in the plane of the ecliptic is a uniform one, while the distribution of the velocities and the directions of the velocities is at random, apart from small changes, due to the variability of the velocity of the earth in its orbit, the total numbers of particles, which are daily swept up by the earth, must remain a constant through all seasons. To an observer at a given geographical latitude there still will appear to exist a seasonal trend. This appears from the same reasoning which is applied to show, that with an at random distribution of the true radiants in the frequency of the meteorites a maximum occurs in autumn. The instantaneous vertex of the earth's motion is in the ecliptic and about 90° West of the sun. Due to the velocity of the earth in its orbit, the apparent radiant of the meteors is always displaced in the sky towards the earth's vertex. So there will be more

radiants in the hemisphere containing the vertex than in the opposite hemisphere. The elevation of the vertex varies with the season. In the Northern geographic latitudes the elevation is at a maximum (about 6 a m) around September 21 st and around this date meteors ar most common. To an observer with Northern latitude minimum activity occurs when the vertex has minimum elevation around March 21 st. Consequently, if the iron dust is connected with meteors in the plane of the ecliptic, the seasonal changes in the amount of iron dust will be such, that a minimum occurs around March. From then on the daily amounts will steadily increase, until a maximum is reached around September 21 st. Afterwards the daily amounts will continually decrease, until the next minimum in March.

In the Southern latitudes the reverse will be the case, the maximum will be in March and the minimum in September.

The total yearly amount of iron dust should be largest in points near the equator. Also in points near the equator two maxima can be expected in March and September respectively. It is difficult to make any prediction about the depths of the troughs and the heights of the maxima, as these depths and heights are determined by the scatter of the radiants around the vertex of the earth's motion. In its turn this scatter depends on the distribution of the velocities and the distribution of the direction of the velocities of the individual particles.

On the other hand the general shape of the curve seems to be pretty well determined. For the latitude of Ankara the maximum should occur in September and the minimum in March. However, it is entirely dubious, whether from the shape of the observed curve it will be possible to discriminate between the case where the true radiants have an at random distribution in the plane of the ecliptic or an at random distribution over the whole surface of the sky.

On the other hand, if from continued observations the maxima and minima of the daily amounts of iron dust appear to occur in September and March respectively, this will indicate the existence of a correlation between the iron dust and the meteors.

§ 8. Case C.

We finally assume the meteors to move in closed orbits around the sun and the plane of the orbits to coincide with or to be near the plane of the solar equator. Obviously two maxima and two minima are to be expected.

The maxima occur when the earth crosses the plane of the solar equator, while the minima are at the time when the earth is at maximum distance from that plane. The maxima and minima will roughly be spaced at three months intervals.

The earth wil pass through the region where the space density of meteoric particles is at a maximum around June 6 th and December 6 th, while the earth is in regions where the space density is at a minimum around March 6 th and September 6 th.

If it were not for the earth's velocity, the maxima and minima of iron dust should therefore occur around June 6 th, December 6 th and March 6 th and September 6 th respectively. But in this case also the observed numbers will be subject to the effect mentioned in § 7. As a result of the velocity of the earth in its orbit, the true radiants of the particles will be shifted in the direction of the instantaneous vertex of the earth's motion and for observation of the particles circumstances are most favourable around September 26 th and most unfavourable around March 26 th. We can only roughly indicate what shape the distribution curve must be expected to have.

Let $F(z)$ indicate the distribution of the meteoric dust with respect to the plane of the solar equator. As analytical form of this function we adopt the expression

$$F(z) = F(o) \exp(-Az^2) \qquad \cdots\cdot(1.8)$$

where z is the perpendicular distance of a particle from the plane of the solar equator and A an unknown constant.

If z is expressed in A. U and the inclination of the solar equator to the plana of the equator is taken to be exactly 7°, we have for any day of the year

$$z = \sin 7^\circ \sin(\lambda_\odot + 105) \qquad \cdots\cdot(2.8)$$

We have no single information about the possible value of the contant A. Therefore the computations were carried through for two values of A. With the first it was supposed that at the maximum distance of the earth from the plane of

the solar equator $F_1(z) = \frac{1}{2} F(o)$ and with the second that in the same circumstances $F_2(z) = \frac{1}{10} F_0$. In these cases the daily amounts of iron dust swept up by the earth but for a constant are as indicated in Table 14.

TABLE 14

Curves F_1 and F_2; curve $R=1+B \sin(\lambda_\odot - 90)$ for B the hypothdical value $B = {}^1/_2$ is adopted; curves $P = F.R$

Date	Curve F_1	Curve F_2	Curve R	Curve $P_1 = F_1 R$	Curve $P_2 = F_2 R$
Jan. 20	0.71	0.32	0.75	0.53	0.24
F. 20	0.52	0.12	0.57	0.30	0.07
M. 20	0.52	0.12	0.50	0.26	0 06
A. 20	0.71	0.32	0.57	0.53	0.24
M. 20	0.95	0.86	0.75	0.71	0.65
J. 20	0.95	0.86	1.00	0.95	0.86
J. 20	0.71	0.32	1.25	0.89	0.40
A. 20	0.52	0.12	1.43	0.74	0.17
S. 20	0.52	0.12	1.50	0.78	0.18
O. 20	0.71	0.32	1.43	1.02	0.46
N. 20	0.95	0.86	1.25	1.19	1.07
D. 20	0.95	0.86	1.00	0.95	0.86

We will represent the yearly variation of the observed relative frequency, due to the changing position of the vertex of the earth's motion by an expression of the form

$$R = 1 + B \sin(\lambda_\odot - q\,0) \qquad \cdots\cdot(3.8)$$

where B is unknown constant ($B < 1$). If for B the entirely hypothetical value $B = 0.5$ is adopted, we find the curve R which is indicated in the fourth column of table 14. This curve could be valid only for a point on the Northern hemisphere.

The observed amounts of iron dust will be proportional to the products

$$P = F \cdot R \qquad \cdots\cdot(4.8)$$

These products are also indicated in table 14, while the resulting curves are graphically represented in fig. 6. It should be

remembered that the numerical values on which the curves in fig. 6 are based, are entirely hypothetical. Still, these curves give some information as to the distribution curve which is to be expected in this case. If there is a fairly large scatter of the individual distances of the particles to plane of the equator

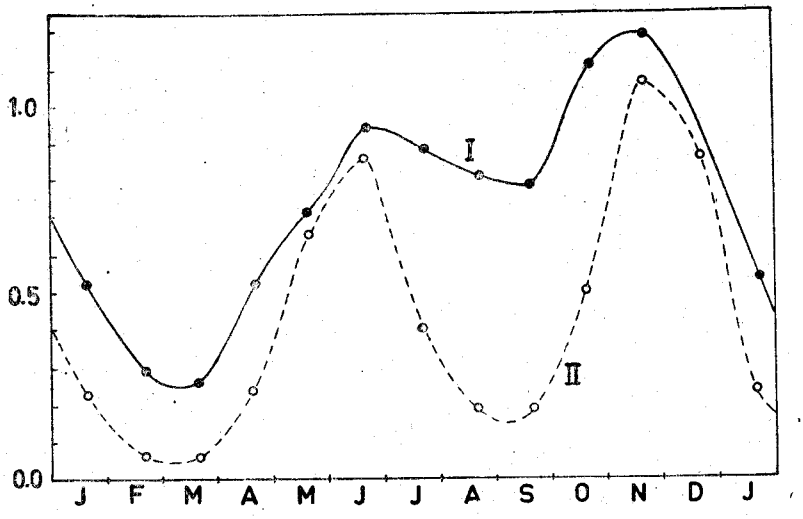

Fig. 6

(curve $F_1 \cdot R$), the maxima will be in June and November, while the minimum between these two maxima is rather shallow. On the other hand if the meteoric material is strongly concentrated towards the plane of the solar equator, pronounced maxima occur in June and November, while these maxima are separated by minima of almost equal depth. In any case the observed distribution will be determined both by the coefficient A in (1.8) and the coefficient B in (3.8).

§ 9. Summary.

1. Assuming that the iron dust which at this Institute has been observed daily to fall on the surface of the earth, is related to the meteors, the seasonal changes in the daily amounts of iron dust should be related to the seasonal changes in the occurrence of meteors.

2. As yet there is no direct evidence that the origin of the iron dust is an extra-terrestial one. For deciding this question

one of the criteria will be whether the seasonal changes in the observed distribution curve corresponds to the curve valid for meteors.

3. From the work of Whipple [12], Prentice [13], Porter [14], Clegg a. o. it has become increasingly certain that the meteors are permanent members of the solar system. Nevertheless, when computing the theoretical distribution curves for the meteors, three possibilities were considered:

A. the iron dust is assumed to be connected with meteors of cosmic origin;

B. The iron dust is assumed to be connected with meteors moving in the plan of the ecliptic;

C. The iron dust is connected with meteors moving in the plane of the solar equator.

4. For each of these three cases the theoretical distribution curves have been computed, but in each case some additional assumptions were found to be necessary. The resulting theoretical curves therefore have no real meaning, but merely indicate what kind of distribution is to be expected. It is hoped that from further observation it will be possible to determine the actual type of the distribution curve and eventually to determine the numerical constants of the arbitrary coefficients which have been introduced.

5. For case A the computations were carried out while assuming that relative to the local system of rest, the interstellar cloud from which the meteors originate, has zero velocity. Each point of the earth's orbit then appears to be intersected by two streams of particles, an incoming and an outgoing one. The radiant of the incoming stream passes through the observer's meridian shortly past midnight, that of the outgoing one shortly before noon. The radiants are confined to narrow belts North and South of the ecliptic and their longitude increases uniformly in the course of the year.

6. The graphical representation of these radiants gives a figure, which at first sight seems closely to resemble that observed by Lovell and Clegg. However, it is impossible to identify these computed radiants with the observed ones. The declina-

tions of the observed radiants are widely different from the computed ones. The distribution of the observed radiants sooner suggests some connection with the plane of the solar equator.

7. If the iron dust is connected with cosmic meteors such as described for case A, the curve giving the seasonal variations will indicate one yearly maximum and one minimum. For the different geographic latitudes the times of maxima and minima are different.

8. If the iron dust is correlated to meteors moving in or near the plane of the ecliptic, for all places in Northern latitudes the maximum will occur at the instant when the instantaneous vertex of the earth's motion has its greatest elevation, that is around September 21 st.

9. If the iron dust is correlated to meteors movings in the plane of the solar equator, two maxima and two minima should occur. The greater the concentration is of the meteoric dust towards the plane of the equator, the more pronounced these maxima and minima will be. There also will be a strong influence of the displacement of the earth's vertex in the course of the year, and the minimum between June and November may almost completely be obliterated.

List of Literature:

1) Whipple F. L. Proc. Am. Phil. Soc **83**, 711, 1940
2) Lovell B. and Clegg J. A. Rdio Astronomy London 1952
3) Hoffmeister C. Die Meteore (Leipzig Akad. Verlag) 1937
4) See 2 5) see 2 6) see 2 7) see 2 8) see 2 9 see 2
10) Prentice J. P. M. Meteors, Phys. Soc. Rep. Prog. Phys. **11**, 389
11) Mc Kinley D. W. R. and Millman P. J. Canad. Jr. Res. **27**, 53, 1949
12) see 1 13) see 10 14) Porter J. G. The Internatioual Astroph. Ser. London 1952

Department of Astronomy
Ankara, August 1954.

Communications de la Faculté des Sciences de l'Université d'Ankara

Table des Matières

Fasc. 1

Tome VII Série A